



Composition dependence of thermoelectric properties of binary narrow-gap $\text{Ga}_{67-x}\text{Ru}_{33+x}$ compound

Y. Takagiwa^{a,*}, J.T. Okada^b, K. Kimura^a

^a Department of Advanced Materials Science, The University of Tokyo, Kiban-toh 502, 5-1-5 Kashiwanoha, Kashiwa-shi, Chiba 277-8561, Japan

^b Department of Space Biology and Microgravity Sciences, Japan Aerospace Exploration Agency, 2-1-1 Sengen, Tshukuba-shi, Ibaraki 305-8505, Japan

ARTICLE INFO

Article history:

Received 25 May 2010

Received in revised form 22 July 2010

Accepted 28 July 2010

Available online 4 August 2010

Keywords:

Thermoelectric material

Narrow-band-gap semiconductor

Ruthenium gallide

Spark plasma sintering

Nowotny chimney-ladder phase

ABSTRACT

The composition and carrier concentration variations of the thermoelectric properties of the binary narrow-gap compound $\text{Ga}_{67-x}\text{Ru}_{33+x}$ have been investigated. The measured samples were synthesized by a combination of arc-melting and spark plasma sintering (SPS), succeeded in crack-free samples. We report that the temperature dependences of the electrical resistivity and Seebeck coefficient of the $\text{Ga}_{67-x}\text{Ru}_{33+x}$ are strongly affected by nominal Ru concentration. The Seebeck coefficients showed large positive values from 170 to 350 $\mu\text{V}\text{K}^{-1}$ at 373 K. Also, large power factors from 2.2 to 3.0 $\text{mW}\text{m}^{-1}\text{K}^{-2}$ were obtained at 773 K. The dimensionless figures of merit ZT beneficially increased with increasing temperature and reached a maximum value of 0.50 at about 773 K.

© 2010 Elsevier B.V. All rights reserved.

1. Introduction

Thermoelectric materials can be used to create devices that generate power through the direct conversion of thermal energy to electrical energy. They have no moving parts and have advantages of maintenance-free, silent, and long-life. Up to now, the low efficiency of energy conversion prevents us from utilizing as commercial use. The evaluation as thermoelectric materials is defined by the dimensionless figure of merit, $ZT = S^2\sigma T/\kappa$, where S , σ , κ , and T are the Seebeck coefficient, the electrical conductivity, the total thermal conductivity, and the temperature, respectively. One of the criteria for the practical applications of thermoelectric materials is that ZT is, at least, above unity. To optimize ZT , search for materials exhibiting large power factor $S^2\sigma$ and low thermal conductivity κ should be necessary. Recently, a large ZT value near of 1.0 has been reported in Si nanowires [1]. While the low-dimensional materials exhibit a high ZT value [1–4], we stress on the importance of bulk materials for practical use in, for example, industrial processes.

Unconventional semiconductors such as FeSi [5] have attracted attention for thermoelectric materials. While alloys composed of metallic constituents are natively expected to be metallic, hybridization between transition metals (TMs) and group III and IV elements, such as Al, Ga, and Si, leads to a band gap in the d bands

near the Fermi level, as confirmed by theoretical calculations [6]. A few hundred meV of narrow-gap near the Fermi level is expected to result in a large absolute value of the Seebeck coefficient, which is desirable to extract a high electric power. Indeed, the Fermi level near the band-edge of a narrow-gap is considered to be suitable for high performance of thermoelectric materials according to the theoretical results [7,8].

In this study, we focus our attention on the binary narrow-gap intermetallic compound Ga_2Ru . The crystal structure of the Ga_2Ru compound is displayed in Fig. 1. They possess the orthorhombic TiSi_2 -type crystal structure, which has the space group $Fddd$ with 24 atoms per unit cell. This compound is one of the Nowotny chimney-ladder (NCL) phases with the valence electron concentration (VEC) ~ 14 [9]. The other promising thermoelectric materials of NCL phases are reported in such as Ru_2Si_3 [10] and $\text{Ru}_{1-x}\text{Re}_x\text{Si}_y$ [11] alloys. The temperature dependence of the electrical conductivity from room temperature to 670 K has been reported by Evers et al. [12], and pioneering studies on the thermoelectric properties of a hot-pressed sample have been reported by Amagai et al. [13]. The maximum ZT value was 0.3 at 780 K [13], however, this value is significantly lower than that required for the practical thermoelectric materials. We have already reported the improvement of the thermoelectric properties of the Ga_2Ru synthesized by a combination of the arc-melting, annealing, and spark plasma sintering (SPS) [14]. The maximum ZT of the arc-melted, annealed, and sintered Ga_2Ru was 0.45 at 773 K [14], which is about one and a half times higher than that of a hot-pressed sample [13]. Same as narrow-band-gap semiconductors such as $\text{ReSi}_{1.75}$ [15], physical properties

* Corresponding author. Fax: +81 4 7136 3759.

E-mail address: takagiwa@phys.mm.t.u-tokyo.ac.jp (Y. Takagiwa).

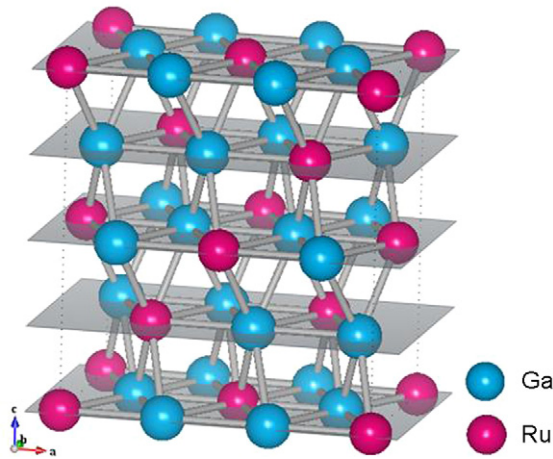


Fig. 1. Crystal structure of Ga_2Ru compound. The blue and magenta spheres indicate Ga and Ru atoms, respectively.

of the Ga_2Ru are very sensitive to the sample's composition, that is, a position of the Fermi level.

In this study, the composition dependence of the thermoelectric properties of the Ga_2Ru compound has been investigated. In addition, we introduce an effective and simple process for synthesizing the Ga_2Ru : a combination of two methods, that is, arc-melting and spark plasma sintering (SPS) process.

2. Experimental and calculation procedures

$\text{Ga}_{67-x}\text{Ru}_{33+x}$ ($x = 0, 0.2, 0.3, 0.4, 0.5, 0.6, 0.7, 0.8, 0.9, 1.0$) (an ideal stoichiometric composition will be $x = 0.3\text{--}0.4$) mother ingots were synthesized by an arc-melting technique under a purified argon atmosphere. The arc-melted mother ingots were crushed to an average particle size of below $20\ \mu\text{m}$. The powder was placed in a carbon die with a diameter of 10 mm for SPS processing on SPS Syntex Inc. (Dr. Sinter. Lab., SPS-5155). The temperature of the specimen was increased from ambient temperature to 873 K in 5 min, and from 873 K to the consolidating temperature of 1223 K in 5 min, and then the temperature was held for 10 min under an argon atmosphere. A pressure of 40 MPa was applied during the heating process. After the SPS treatment, the specimen was cooled to 873 K under a pressure of 40 MPa, and the pressure was released under 873 K. The phase-identification and the structure refinement of the samples were performed by powder X-ray diffraction (XRD) measurements with $\text{Cu K}\alpha$ radiation and the Rietveld analysis. The microstructures of the synthesized samples were examined using scanning electron microscope (SEM), and the local compositions were analyzed by electron probe micro-analysis (EPMA). The electrical conductivity and Seebeck coefficient were measured in a helium atmosphere at temperatures between 373 and 973 K by the four-probe method and the steady-state temperature gradient method, respectively. The thermal conductivity was obtained by measuring the density using a helium pycnometer at room temperature, and the specific heat and thermal diffusivity were measured from 300 to 973 K by the laser flash method. Hall coefficient measurements were performed at room temperature. Debye temperatures were calculated from the transverse and longitudinal sound velocities measured by the ultrasonic pulse echo method (Nihon Matech Corp., Echometer 1062).

In order to obtain the density of states (DOS) of the Ga_2Ru , we performed the first-principle band-structure calculations by utilizing the package program of WIEN2k [16] with the Full Potential Linearized Augmented Plane Wave (FLAPW) method. The lattice constants and atomic positions determined by the Rietveld analysis were used for the calculation.

3. Sample characterization

Fig. 2 shows experimental and calculated XRD patterns of the $\text{Ga}_{67-x}\text{Ru}_{33+x}$ ($x = 0, 0.2, 0.3, 0.4, 0.5, 0.6, 0.7, 0.8, 0.9, 1.0$) compounds. Almost single phases are observed except for the samples with $x = 0, 0.8, 1.0$, which agrees well with the calculated pattern (k). As there is no significant difference in XRD patterns between arc-melted, annealed, and sintered sample [14] and arc-melted and sintered sample (present sample preparation), we selected more simple process for synthesizing the Ga_2Ru compound. The effect of

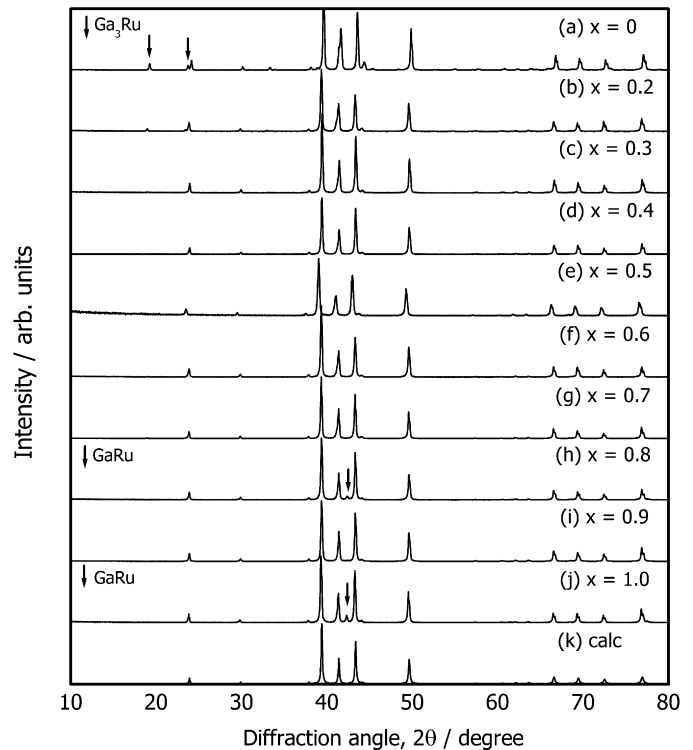


Fig. 2. X-ray diffraction patterns of $\text{Ga}_{67-x}\text{Ru}_{33+x}$: (a) $x = 0$, (b) $x = 0.2$, (c) $x = 0.3$, (d) $x = 0.4$, (e) $x = 0.5$, (f) $x = 0.6$, (g) $x = 0.7$, (h) $x = 0.8$, (i) $x = 0.9$, (j) $x = 1.0$ compounds. Pattern (k) is a calculated pattern. Arrows show the peaks of secondary phases of Ga_3Ru and GaRu .

the sample preparation process on the thermoelectric properties will be discussed in Section 7.

Fig. 3(a and b) shows the typical example of the secondary electron (SEI) and back scattered electron (BEI) images of $\text{Ga}_{66.7}\text{Ru}_{33.3}$ ($x = 0.3$) compound. There are no visible cracks which should decrease the electrical conductivity from Fig. 3(a). In addition, the sample's composition is uniform confirmed by BEI image as shown in Fig. 3(b). This trend is same for all samples.

4. Electronic structure and transport properties

Fig. 4 shows the electronic density of states (DOS) of the stoichiometric Ga_2Ru compound obtained by WIEN2k package program [16]. We can realize the formation of a narrow-band-gap near the Fermi energy E_F . The overall shape of the DOS is consistent with the previous reports [17–19]. Similarly to the isostructural Al_2Ru compound, hybridization between Ga sp and Ru d orbitals, along with some charge transfer, will be the origin of the gap [6]. The inset shows the DOS of vicinity of E_F of the Ga_2Ru compound. About 0.3 eV of narrow-gap near the E_F is observed, and this value is comparable to the experimentally observed value of 0.36 eV of the sintered Ga_2Ru sample [14].

The electrical resistivities ρ of the $\text{Ga}_{67-x}\text{Ru}_{33+x}$ compounds from 373 to 973 K are plotted in Fig. 5. The temperature dependence of ρ is strongly affected by the nominal Ru composition x . ρ of the $\text{Ga}_{67-x}\text{Ru}_{33+x}$ compounds exhibits semiconducting behavior and varies from 1800 ($x = 0.9$) to 28,000 $\mu\Omega\ \text{cm}$ ($x = 0$ and 0.5) at 373 K. This semiconducting temperature dependence of ρ is consistent with the previous reports of the Ga_2Ru [13,14]. It should be noted here that the activation energy Δ of the stoichiometric sample with $x = 0.4$ is about 0.16 eV from the Arrhenius plot (not shown here). This yields $E_g = 2\Delta \sim 0.32\ \text{eV}$ for the band gap, which is consistent with the result of band-structure calculation,

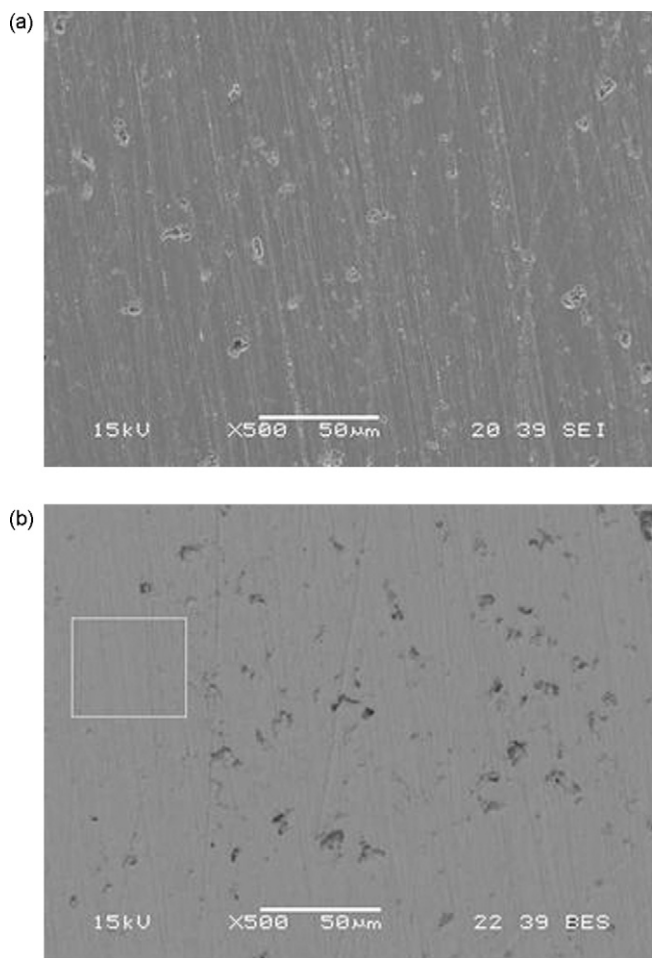


Fig. 3. (a) Secondary electron (SEI) and (b) backscattered electron (BSE) images of $\text{Ga}_{66.7}\text{Ru}_{33.3}$ ($x=0.3$) compound.

as shown in Fig. 4. The temperature dependence and magnitude of ρ are not systematically dependent of x , similarly to the Seebeck coefficient as discussed in the next paragraph. The magnitude of ρ can be understood by the varying carrier concentrations.

The Seebeck coefficients S of the $\text{Ga}_{67-x}\text{Ru}_{33+x}$ compounds from 373 to 973 K are plotted in Fig. 6. A large positive S over $120 \mu\text{VK}^{-1}$ was observed over the wide temperature range from 373 to 973 K.

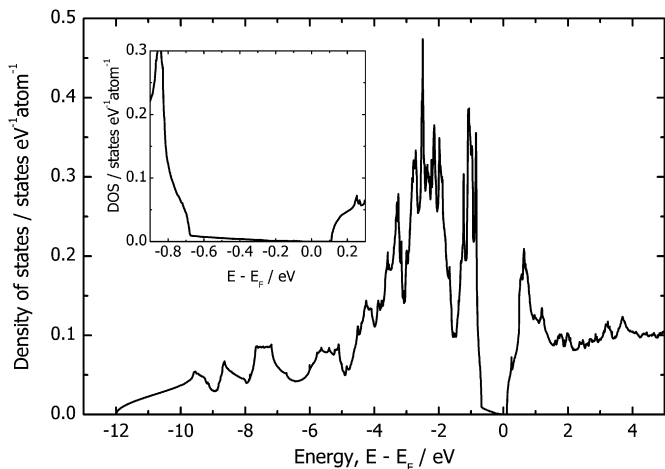


Fig. 4. Electronic density of states (DOS) of stoichiometric Ga_2Ru compound using FLAPW method by WIEN2k [12]. The inset shows the DOS of the vicinity of the Fermi energy.

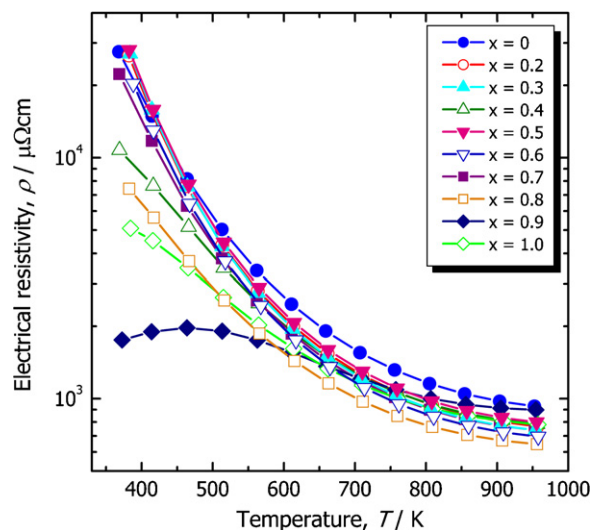


Fig. 5. Electrical resistivity ρ as a function of temperature T for $\text{Ga}_{67-x}\text{Ru}_{33+x}$ ($x=0, 0.2, 0.3, 0.4, 0.5, 0.6, 0.7, 0.8, 0.9, 1.0$) compounds.

The maximum S value deviates widely from 170 to $350 \mu\text{VK}^{-1}$. These variations are characterized by the electronic structure with a narrow-band-gap, as shown in Fig. 4. The temperature dependences and magnitudes of S and ρ of the sample with $x=0.9$ is quite similar to the previous reported data of a hot-pressed sample by Amagai et al. [13]. Especially, the absolute values of S and ρ under 600 K are quite sensitive to the nominal Ru concentration x . It should be noted here that the sample composition is different from the nominal composition because the mass reduction (maximum 3%) was observed during the arc-melting process. To clarify the composition variations of ρ or σ , we investigated the Hall carrier concentration n_H at 300 K dependence of the electrical conductivity $\sigma_{300\text{K}}$, as shown in Fig. 7. While the carrier concentrations at 373 K are larger than that at 300 K, we also plotted S at 373 K to roughly understand the carrier concentration dependence of S .

Given that the room-temperature Hall coefficients of the $\text{Ga}_{67-x}\text{Ru}_{33+x}$ compounds are positive, it is obvious that holes dominantly contribute to the conduction. This result is consistent with the Seebeck coefficients and the band-structure calculations, which predicts that the Ga_2Ru compound is a narrow-band-gap semiconductor with light hole and heavier electron pockets [17–19].

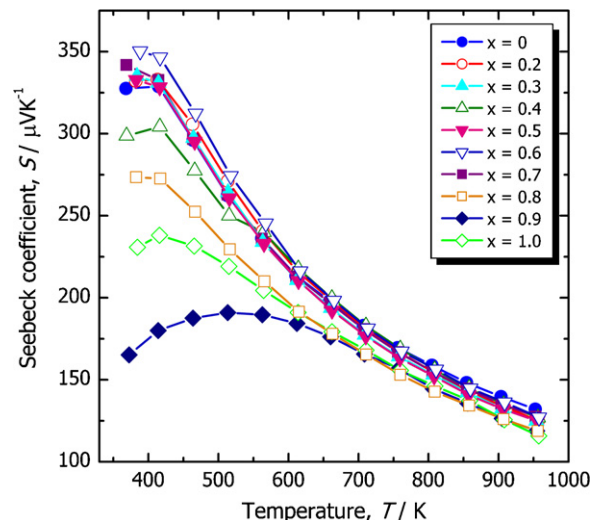


Fig. 6. Seebeck coefficient S as a function of temperature T for $\text{Ga}_{67-x}\text{Ru}_{33+x}$ compounds.

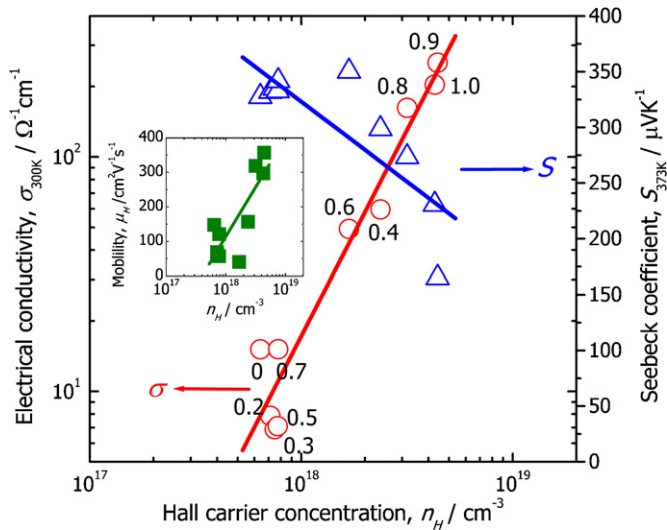


Fig. 7. Electrical conductivity $\sigma_{300\text{K}}$ and Seebeck coefficient $S_{373\text{K}}$ as a function of Hall carrier concentration n_{H} at 300 K for $\text{Ga}_{67-x}\text{Ru}_{33+x}$ compounds. The value of x is written near each circle of $\sigma_{300\text{K}}$. The inset shows the n_{H} dependence of Hall carrier mobility μ_{H} at room temperature. The solid lines are drawn to guide the eye.

The Hall carrier concentration n_{H} at room temperature tends to increase from 6.4×10^{17} to $4.4 \times 10^{18} \text{ cm}^{-3}$, indicating the E_{F} shifts to lower energy level with increasing Ru concentration x . While the electrical conductivity $\sigma_{300\text{K}}$ at 300 K increases with increasing n_{H} , Seebeck coefficient $S_{373\text{K}}$ at 373 K decreases with increasing n_{H} . This can be understood qualitatively by the following equations.

$$\sigma = \frac{ne^2\tau}{m^*} \quad (1)$$

$$S = \frac{k_{\text{B}}}{e} \left(-\log \frac{n}{n_0} + \delta \right) \quad (2)$$

$$n_0 = \frac{1}{2} \left(\frac{2mk_{\text{B}}T}{\pi\hbar^2} \right)^{3/2} \quad (3)$$

Here n , e , τ , k_{B} , m^* and m represent the carrier concentration, the unit charge of electron, the relaxation time, the Boltzmann constant, the effective mass, and the free electron mass, respectively. However, $\sigma_{300\text{K}}$ do not change linearly with varying n_{H} . In this case, m^* and/or τ change markedly with changing nominal Ru concentration x from the data of the Hall carrier mobility μ_{H} , expressed as $\mu_{\text{H}} = R_{\text{H}}/\rho$, varying from 41 to $357 \text{ cm}^2 \text{ V}^{-1} \text{ s}^{-1}$ at room temperature. When E_{F} shifts to lower energy with increasing x , a substantial increase in the DOS at E_{F} should decrease the effect of scattering carriers by disorders in spite of increasing chemical disorder introduced by changing Ga and Ru concentrations, which leads to an increase in μ_{H} with increasing n_{H} .

The power factors $S^2\sigma$ of the $\text{Ga}_{67-x}\text{Ru}_{33+x}$ compounds from 373 to 973 K are plotted in Fig. 8. $S^2\sigma$ increases with increasing temperature and reaches maximum values $S^2\sigma_{\text{max}}$ at about 773 K, and then decreases up to 973 K for all samples. $S^2\sigma_{\text{max}}$ exhibits large values from 2.2 to $3.0 \text{ mW m}^{-1} \text{ K}^{-2}$ whose values are much higher than those of isostructural Al_2Ru compound [14,20,21]. Also, these $S^2\sigma_{\text{max}}$ are sufficiently high values which are comparable with the practical thermoelectric materials.

5. Thermal conductivity

The total thermal conductivity κ_{total} of the $\text{Ga}_{67-x}\text{Ru}_{33+x}$ compounds from 300 to 973 K are shown in Fig. 9(a). κ_{total} first decreases with increasing temperature up to 600 K, and then increases with increasing temperature; this is mainly brought by the increase in

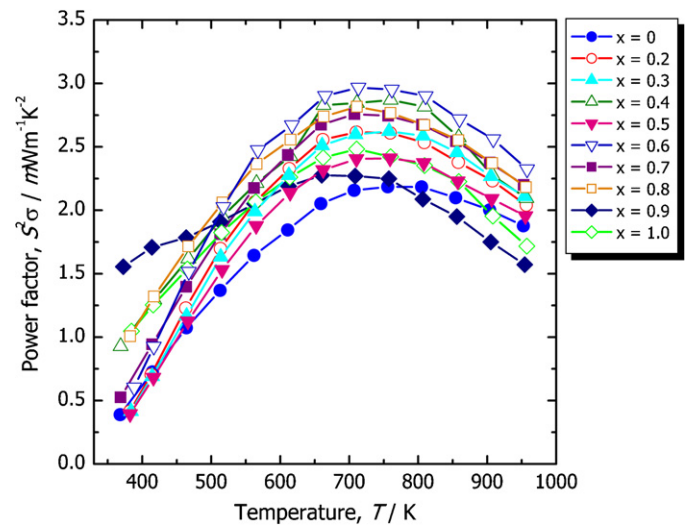


Fig. 8. Power factor $S^2\sigma$ as a function of temperature T for $\text{Ga}_{67-x}\text{Ru}_{33+x}$ compounds.

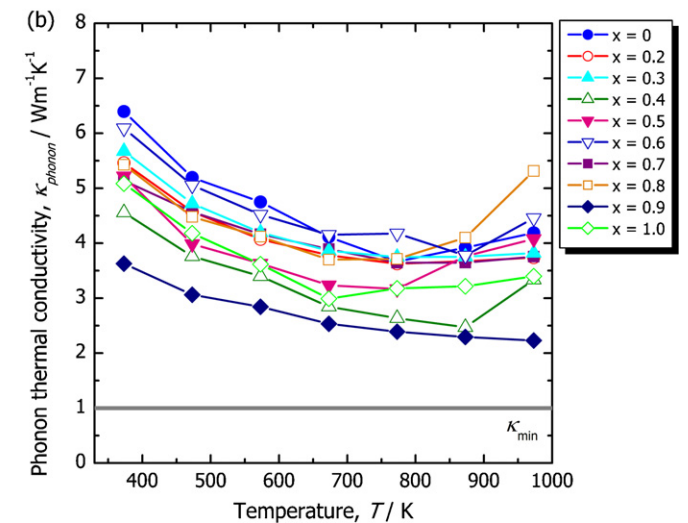
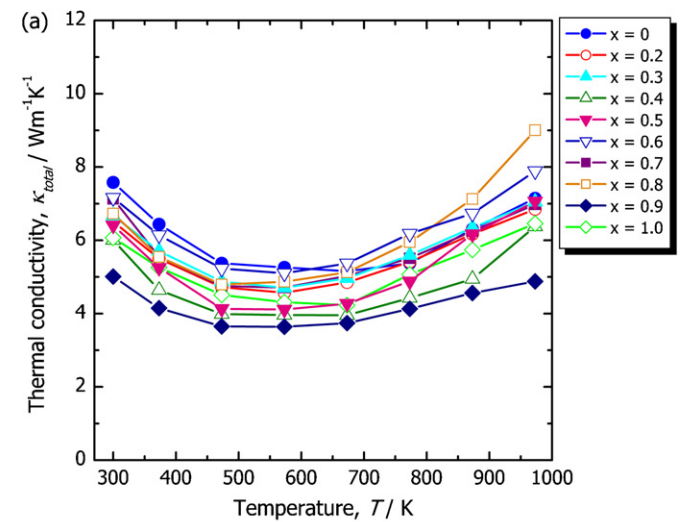


Fig. 9. (a) Total thermal conductivity κ_{total} and (b) lattice thermal conductivity $\kappa_{\text{phonon}} (= \kappa_{\text{total}} - \kappa_{\text{electron}})$ as a function of temperature T for $\text{Ga}_{67-x}\text{Ru}_{33+x}$ compounds. Electron thermal conductivity κ_{electron} were estimated using by the Wiedemann–Franz law. The minimum lattice thermal conductivity κ_{min} is also shown in (b).

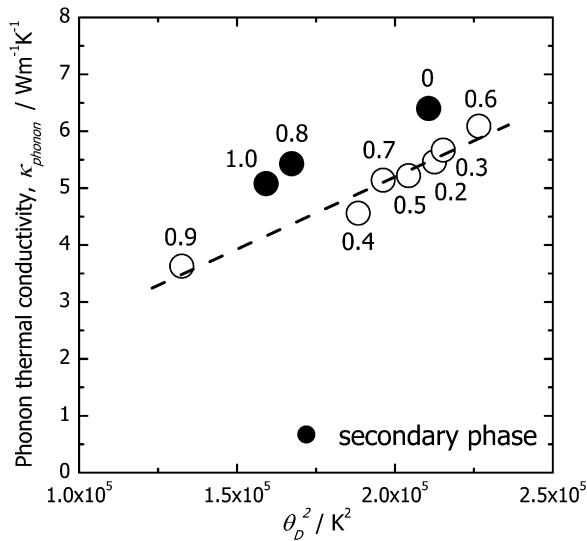


Fig. 10. Phonon thermal conductivity κ_{phonon} as a function of the square of Debye temperature θ_D for $\text{Ga}_{67-x}\text{Ru}_{33+x}$ compounds. Closed circles represent the samples ($x=0, 0.8, 1.0$) with a secondary phase. The value of x is written near each circle of κ_{phonon} . The dashed line is drawn to guide the eye.

κ_{electron} as estimated by the Wiedemann–Franz law expressed by the following equation:

$$\kappa_{\text{electron}} = L_0 \sigma T, \quad (4)$$

where L_0 is the Lorentz number. We assumed L_0 to be $2.45 \times 10^{-8} \text{ V}^2 \text{ K}^{-2}$. It was observed that Ru-rich samples with heavier atomic weight have the lower lattice components κ_{phonon} ($=\kappa_{\text{total}} - \kappa_{\text{electron}}$) as shown in Fig. 9(b). Also, we calculated the minimum lattice thermal conductivity κ_{min} for the Ga_2Ru compound using the model proposed by Cahill et al. [22]. The calculated κ_{min} is about $1.0 \text{ W m}^{-1} \text{ K}^{-1}$ above 373 K as described in Fig. 9(b). It seems that both κ_{total} and κ_{phonon} have not exact correlation with the nominal composition, similarly to the behaviors of σ and S .

In Fig. 10, κ_{phonon} is plotted as a function of the square of the Debye temperature θ_D calculated by the sound velocities for the $\text{Ga}_{67-x}\text{Ru}_{33+x}$ compounds. Closed circles represent the samples ($x=0, 0.8, 1.0$) with secondary phase. The dashed line is drawn to guide the eye. As for the samples of single phase, κ_{phonon} decreases systematically with decreasing θ_D . κ_{phonon} and θ_D are expressed as

$$\kappa_{\text{phonon}} = \frac{1}{3} C v_S^2 \tau_{\text{phonon}} = \frac{1}{3} C \frac{a^2 K}{M} \tau_{\text{phonon}}, \quad (5)$$

$$\theta_D = \left(\frac{\hbar v_S}{k_B} \right) (6\pi^2 n)^{\frac{1}{3}}, \quad (6)$$

where C , v_S , τ_{phonon} , a , K , M , and n are the specific heat, the sound velocity, the distance of atoms, the spring constant, the mass, the relaxation time of phonon, and the number of atoms per volume ($=N/V$), respectively. κ_{phonon} of the samples of single phase has a strong correlation with θ_D^2 . In this case, the effect of decreasing K/M attributed to an increase of Ru concentration x is dominant factor for decreasing κ_{phonon} . Substitution of multiple elements with different masses will reduce κ_{phonon} via induced mass fluctuations and strain field effects [23,24].

6. Estimation of figure of merit

Finally, we present the dimensionless figure of merit ZT of the $\text{Ga}_{67-x}\text{Ru}_{33+x}$ compounds from 373 to 973 K in Fig. 11. ZT increases monotonically up to 773 K, and then decreases with increasing temperature. The maximum ZT value ZT_{max} of the $\text{Ga}_{67-x}\text{Ru}_{33+x}$ compounds is 0.50 at 773 K for the sample with $x=0.4$. This value

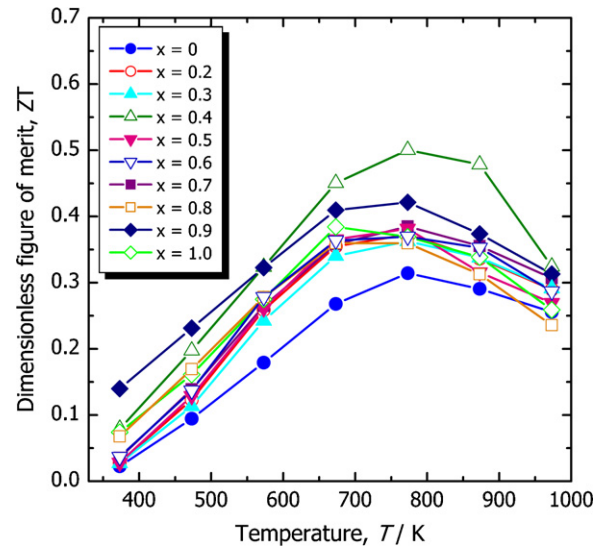


Fig. 11. Dimensionless figure of merit ZT as a function of temperature T for $\text{Ga}_{67-x}\text{Ru}_{33+x}$ compounds.

is much higher than that of the isostructural Al_2Ru compound: SPS samples ($ZT_{\text{max}} = 0.20$ [14] at 773 K and $ZT_{\text{max}} = 0.17$ [21] at 870 K) and a hot-pressed sample ($ZT_{\text{max}} = 0.07$ at 800 K) [20]. Also, this nominal composition ($\text{Ga}_{66.6}\text{Ru}_{33.4}$) is near the stoichiometric composition. In this case, the sample without chemical disorder exhibits the highest inherent ZT value. This will be confirmed from a hole doping effect on the thermoelectric properties upon substitution of Re for Ru atoms [25].

To realize the maximum ZT value of the Ga_2Ru compound, we calculated the theoretical maximum ZT value, assuming that the mean-free path of phonons is limited to the distance of atoms. The minimum lattice thermal conductivity κ_{min} is about $1.0 \text{ W m}^{-1} \text{ K}^{-1}$. Assuming that the power factor maintains $3.0 \text{ mW m}^{-1} \text{ K}^{-2}$, the theoretical maximum ZT value is ~ 0.77 using the ideal minimum thermal conductivity ($=\kappa_{\text{min}} + \kappa_{\text{electron}}$). This indicates that this Ga_2Ru compound will be a promising candidate for new thermoelectric materials.

7. Effect of sample preparation process on ZT value

We briefly comment on the sample preparation process on the thermoelectric properties, that is, ZT value of the Ga_2Ru compound. In our earlier studies [14], measured Ga_2Ru samples were prepared by the following procedure. The mother ingots were synthesized by an arc-melting technique and the ingots were annealed at 1273 K for 24 h (arc \rightarrow anneal [called process A]). Then the sintered samples were prepared by SPS method (arc \rightarrow anneal \rightarrow SPS [called process B]). The maximum ZT value was ~ 0.45 for the $\text{Ga}_{67}\text{Ru}_{33}$ ($x=0$) compound [14]. On the other hand, the arc-melted ingot was sintered by SPS without annealing in this study (arc \rightarrow SPS [called process C]). Fig. 12 shows the temperature dependence of ZT value for the $\text{Ga}_{67}\text{Ru}_{33}$ ($x=0$) samples synthesized by different sample's preparation processes. The process A sample showed the lower ZT value in overall temperatures than those of the samples synthesized by the other processes. This is due to the fact that the process A sample contains a lot of cracks and pores introduced by the arc-melting process, which should decrease σ . The process B sample has the highest ZT value, which means that the former sample process (process B) seems to be more favorable than the present one (process C).

In order to understand the difference in ZT value, we analyzed the local compositions of some samples synthesized by processes

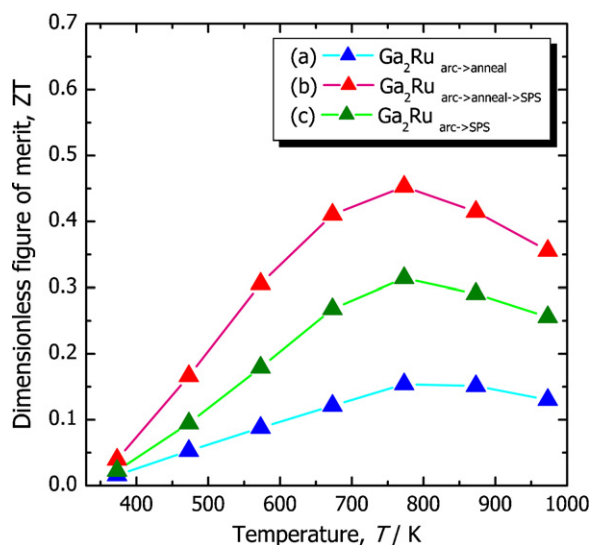


Fig. 12. Dimensionless figure of merit ZT as a function of temperature T for $\text{Ga}_{67}\text{Ru}_{33}$ ($x=0$) compounds synthesized by (a) arc-melting and annealing process, (b) arc-melting, annealing, and sintering process, and (c) arc-melting and sintering process.

Table 1

Averaged microprobe compositions of $\text{Ga}_{67-x}\text{Ru}_{33+x}$ compounds ($x=0, 0.4$) synthesized by process B and C.

Sample	Process B	Process C
$x=0$	$\text{Ga}_{68.2\pm 0.4}\text{Ru}_{31.8\pm 0.4}$	$\text{Ga}_{68.4\pm 0.2}\text{Ru}_{31.6\pm 0.2}$
$x=0.4$	$\text{Ga}_{69.0\pm 1.0}\text{Ru}_{31.0\pm 1.0}$	$\text{Ga}_{68.3\pm 0.5}\text{Ru}_{31.7\pm 0.5}$

B and C using electron probe micro-analysis (EPMA). Table 1 lists the averaged microprobe compositions of the $\text{Ga}_{67-x}\text{Ru}_{33+x}$ ($x=0, 0.4$) synthesized by processes B and C. One can easily realize that the averaged microprobe sample's compositions deviate slightly with different sample preparation processes. About 0.2–0.3 at.% increases of Ru concentration are considered to exist for the process B comparing to the C in both the samples with $x=0$ and 0.4, which is not clear in Table 1 because of large inhomogeneity on the composition for the process B. Considering that the mother ingots are same for the processes B and C, the sample's compositions will be changed by the annealing process at 1273 K for 24 h. On the basis of the composition dependence of ZT values, as shown in Fig. 11, only 0.1 at.% of composition's difference affects the maximum ZT value. While the bulk densities were almost same, that is, 9.02 and 9.04 g cm^{-3} for the sample with process B and C, respectively, we can conclude that the sample's compositions have critical influence on the ZT value rather than the sample preparation process. Another remarkable feature is the sample's composition deviation. The composition deviation in the process C is smaller than that in the process B. This is one of the main reasons to select the process C for synthesizing the Ga_2Ru compound in this study. The other is the more simple process without an annealing process.

8. Conclusions

In this study, the composition dependence of the thermoelectric properties and the dimensionless figures of merit ZT of the $\text{Ga}_{67-x}\text{Ru}_{33+x}$ compounds with various Ru concentrations $x=0, 0.2, 0.3, 0.4, 0.5, 0.6, 0.7, 0.8, 0.9, 1.0$ were systematically investigated.

The new synthesizing process of the Ga_2Ru compound has been tested: that is, the arc-melted and sintered process. The electrical conductivity and Seebeck coefficient were strongly affected by the nominal sample's composition, and these changes were identified by varying the carrier concentration observed from Hall coefficient measurements. As for the $\text{Ga}_{66.6}\text{Ru}_{33.4}$ ($x=0.4$) sample, the maximum ZT value of 0.50 was obtained, indicating that the sample without chemical disorder introduced by changing Ga and Ru concentrations from stoichiometric composition exhibited the highest inherent ZT value in the Ga_2Ru compound.

The theoretical maximum ZT value of the Ga_2Ru compound is ~ 0.77 , as estimated using the ideal minimum thermal conductivity ($=\kappa_{\text{min}} + \kappa_{\text{electron}}$). This indicates that this Ga_2Ru compound as well as the Al_2Ru compound with TiSi_2 -type crystal structure will be new thermoelectric materials. Further enhanced ZT value will be achieved by the reduction of the lattice thermal conductivity κ_{phonon} upon an alloying effect and the increase of scattering phonons by fine grain boundaries [26].

Acknowledgements

This work is partly supported by the Thermal & Electric Energy Technology Foundation (TEET) and KAKENHI No. 21860021 from JSPS and Scientific Research on Priority Areas of New Materials Science Using Regulated Nano Spaces, KAKENHI No. 19051005 from MEXT.

References

- [1] A.I. Boukail, Y. Bunimovich, J. Tahir-Kheli, J.K. Yu, W.A. Goddard III, J.R. Heath, Nature 451 (2008) 168.
- [2] L.D. Hicks, M.S. Dresselhaus, Phys. Rev. B 47 (1993) 12727.
- [3] R. Venkatasubramanian, E. Siivola, T. Colpitts, B. O'Quinn, Nature 413 (2000) 597.
- [4] T.C. Harman, M.P. Walsh, B.E. Laforge, G.W. Turner, J. Electron. Mater. 34 (2005) L19.
- [5] Z. Schlesinger, Z. Fisk, H.-T. Zhang, M.B. Maple, J.F. DiTusa, G. Aeppli, Phys. Rev. Lett. 71 (1993) 1748.
- [6] M. Weinert, R.E. Watson, Phys. Rev. B 58 (1998) 9732.
- [7] J.S. Tse, D.D. Klug, in: D.M. Rowe (Ed.), Thermoelectrics Handbook Macro to Nano, Taylor & Francis, Boca Raton, 2006, Chapter 8-1-27.
- [8] T. Takeuchi, Mater. Trans. 50 (2009) 2359.
- [9] D.C. Fredrickson, S. Lee, R. Hoffmann, Inorg. Chem. 43 (2004) 6159.
- [10] B.A. Simkin, Y. Hayashi, H. Inui, Intermetallics 13 (2005) 1225.
- [11] K. Kishida, A. Ishida, T. Koyama, S. Harada, N.L. Okamoto, K. Tanaka, H. Inui, Acta Mater. 57 (2009) 2010.
- [12] J. Evers, G. Oehlinger, H. Meyer, Mater. Res. Bull. 19 (1984) 1177.
- [13] Y. Amagai, A. Yamamoto, C.-H. Lee, H. Ohara, K. Ueno, T. Iida, Y. Takanashi, Papers of Technical Meeting on Frontier Technology and Engineering, IEE Japan, vol. FTE-05, 2005, 41 pp. (in Japanese).
- [14] Y. Takagiwa, Y. Matsubayashi, A. Suzumura, J.T. Okada, K. Kimura, Mater. Trans. 51 (2010) 988.
- [15] A. Qiu, L. Zhang, A. Shan, J. Wu, Phys. Rev. B 77 (2008) 205207.
- [16] P. Blaha, K. Schwarz, G. Madsen, D. Kvasnicka, J. Luitz, An Augmented Plane Wave + Local Orbitals Programs for Calculating Crystal Properties, Techn. Universität Wien, 2001.
- [17] S.E. Burkov, S.N. Rashkeev, Solid State Commun. 92 (1994) 525.
- [18] D.N. Manh, G. Trambly de Laissardiere, J.P. Julien, D. Mayou, F. Cyrot-Lackmann, Solid State Commun. 82 (1992) 329.
- [19] M. Springborg, R. Fischer, J. Phys.: Condens. Matter 10 (1998) 701.
- [20] D. Mandrus, V. Keppens, B.C. Sales, J.L. Sarrao, Phys. Rev. B 58 (1997) 3712.
- [21] S. Takahashi, H. Muta, K. Kurosaki, S. Yamanaka, J. Alloy Compd. 493 (2010) 17.
- [22] D.G. Cahill, S.K. Watson, R.O. Pohl, Phys. Rev. B 46 (1992) 6131.
- [23] Q. Shen, L. Chen, T. Goto, T. Hirai, J. Yang, G.P. Meisner, C. Uher, Appl. Phys. Lett. 79 (2001) 4165.
- [24] J. Yang, G.P. Meisner, L. Chen, Appl. Phys. Lett. 85 (2004) 1140.
- [25] Y. Takagiwa, J.T. Okada, K. Kimura, J. Electron. Mater. (under review).
- [26] K. Hasezaki, T. Hamachiyo, M. Ashida, T. Ueda, T. Noda, Mater. Trans. 51 (2010) 863.